

Unraveling the structural basis for the unusually rich association of human leukocyte antigen DQ2.5 with class-II-associated invariant chain peptides

Thanh-Binh Nguyen^{¶§1}, Priya Jayaraman^{§1}, Elin Bergseng^Δ, Mallur S. Madhusudhan^{¶1}, Chu-Young Kim^{†‡#2}, and Ludvig M. Sollid^{Δ3}

From the [†]Department of Chemistry, University of Texas at El Paso, El Paso, Texas 79968, [‡]School of Pharmacy, University of Texas at El Paso, El Paso, Texas 79968, [#]NUS Synthetic Biology for Clinical and Technological Innovation, Life Sciences Institute, National University of Singapore, 117456 Singapore, the [§]Department of Biological Sciences, National University of Singapore, Singapore 117543, the [¶]Bioinformatics Institute, Singapore 138671, the ^ΔIndian Institute of Science Education and Research, Pune 411008, India, and the ^ΔCentre for Immune Regulation and Department of Immunology, University of Oslo and Oslo University Hospital, N-0372 Oslo, Norway

¹ These authors contributed equally to this work.

² To whom correspondence should be addressed: Department of Chemistry, University of Texas at El Paso, 1852 Hawthorne Street, El Paso, TX 79902. Tel.: 915-747-6935; Fax: 915-747-5748; E-mail: ckim7@utep.edu.

³ To whom correspondence should be addressed: Centre for Immune Regulation and Dept. of Immunology, Oslo University Hospital-Rikshospitalet, N-0372 Oslo, Norway. Tel.: 47-23073811; Fax: 47-23073510; E-mail: l.m.sollid@medisin.uio.no.

Keywords: CLIP, major histocompatibility complex, celiac disease, type 1 diabetes, HLA-DQ, HLA-DM

Abstract

Human leukocyte antigen (HLA)-DQ2.5 (DQA1*05/DQB1*02) is a class II major histocompatibility complex protein associated with both type 1 diabetes and celiac disease. One unusual feature of DQ2.5 is its high class-II-associated invariant chain peptide (CLIP) content. Moreover, DQ2.5 preferentially binds the non-canonical CLIP2 over the canonical CLIP1. To better understand the structural basis of DQ2.5's unusual CLIP association characteristics, better insight into the DQ2.5–CLIP complex structures is required. To this end, we determined the X-ray crystal structure of the HLA-DQ2.5–CLIP1 and HLA-DQ2.5–CLIP2 complexes at 2.73 Å and 2.20

Å, respectively. We found that HLA-DQ2.5 has an unusually large P4 pocket and a positively charged peptide-binding groove that together promote preferential binding of CLIP2 over CLIP1. An α 9- α 22- α 24- α 31- β 86- β 90 hydrogen bond network located at the bottom of the peptide binding groove, spanning from the P1 to P4 pockets, renders the residues in this region relatively immobile. This hydrogen bond network, along with a deletion mutation at α 53, may lead to HLA-DM (DM) insensitivity in HLA-DQ2.5. A molecular dynamics simulation experiment reported here and recent biochemical studies by others support this hypothesis. The diminished DM sensitivity is the likely reason for the CLIP-rich phenotype of HLA-DQ2.5.

associated MHCII proteins consist of one α -chain and one β -chain whose interface forms the peptide binding groove. Humans express three MHCII isotypes; HLA-DR, HLA-DP, and HLA-DQ, all of which are encoded on chromosome 6. Newly synthesized MHCII proteins associate with a

Introduction

Class II major histocompatibility complex (MHCII) proteins present foreign peptides to T cell receptors of CD4⁺ T cells (1). The membrane

chaperone protein called the invariant chain (Ii) and form a nonameric complex ($\alpha_3\beta_3\text{Ii}_3$) in the endoplasmic reticulum (2). This complex formation prevents indiscriminate peptide loading onto the nascent MHCII and also targets the nascent MHCII to the endosome for further processing (3). Once in the endosome, the MHCII bound Ii is progressively proteolyzed until only a short fragment called class-II-associated invariant chain peptide (CLIP) remains attached to the MHCII peptide binding groove (4). Subsequently, CLIP is catalytically released by HLA-DM (DM) and is replaced with exogenous peptides for CD4⁺ T cell examination after transport to the cell surface (5). In addition to CLIP removal, DM also carries out peptide editing by catalyzing the release of low affinity peptides (5,6). Currently, three MHC binding regions have been identified in Ii; the canonical CLIP1 (residues 83-101), non-canonical CLIP2 (residues 92-107), and non-canonical CLIP3 (residues 98-111) (**Fig. 1**). Most mouse and human MHCII associate exclusively with CLIP1 (5). So far only DQ2.2, DQ2.5, DQ7.5, and DQ8 have been shown to bind both CLIP1 and CLIP2 (7-9). DQ7.5 binds CLIP1, CLIP2, and CLIP3 (9). Interestingly, all human MHCII alleles that bind CLIP2 or CLIP3 are associated with one or more autoimmune diseases; Celiac disease (DQ2.2, DQ2.5, DQ7.5 and DQ8) (10-12) and type 1 diabetes (DQ2.5 and DQ8) (11,12).

DQ2.5 is associated with celiac disease, an autoimmune-like disorder caused by a harmful immune response to ingested wheat gluten and similar proteins from rye and barley (13). Approximately 95% of celiac disease patients express DQ2.5 that is encoded by the DQA1*05 and DQB1*02 genes (14). These alleles are found on the DR3-DQ2 haplotype (*cis* configuration) and also in the heterozygous combination of DR5-DQ7/DR7-DQ2 haplotypes (*trans* configuration). The gluten-specific CD4⁺ T cells of celiac disease patients recognize a diverse set of gluten epitopes when they are presented in the context of DQ2.5 but not in the context of other MHCII molecules (15-18). One unusual phenotype of DQ2.5 is its high CLIP content. In DQ2.5 expressing B lymphoblastoid cells, CLIP1 and CLIP2 combined accounts for up to 53% of endogenous displayed peptides (7-9,19).

Generally, CLIP accounts for only about 10% of MHCII displayed peptides (20). Moreover, DQ2.5 preferentially binds the non-canonical CLIP2 over the canonical CLIP1 (7,8). The CLIP-rich phenotype of HLA-DQ2.5 was explained by the MHCII-CLIP being poor substrates for HLA-DM (8,21). In order to better understand the structural basis of the unusual CLIP association characteristics of DQ2.5, we have determined the DQ2.5-CLIP1 complex and DQ2.5-CLIP2 complex crystal structures.

Results

DQ2.5-CLIP1 and DQ2.5-CLIP2 crystal structures

The crystal structure of DQ2.5-CLIP1 (PDB ID: 5KSU) and DQ2.5-CLIP2 (PDB ID: 5KSV) were solved to 2.73 Å and 2.20 Å resolution, respectively (**Fig. 2**). In both structures the β 105-112 loop was not modelled due to missing electron density. In the DQ2.5-CLIP1 structure, side chain of α 75, α 158, α 172, β 22 and β 135 were not modelled due to ambiguous electron density. Data collection and refinement statistics are presented in Table 1. Conformation of the DQ2.5 protein in the DQ2.5-CLIP1 and DQ2.5-CLIP2 structures are highly similar to each other (C^α RMSD of 1.09Å) and to the DQ2.5 conformation in the DQ2.5-gliadin- α 1a (PDB ID: 1S9V) (15) and DQ2.5-gliadin- α 2 (PDB ID: 4OZF, 4OZG, and 4OZH) (16) structures (C^α RMSD ranging from 0.57 to 1.27 Å). In the current structures, CLIP1 and CLIP2 have highly similar main chain conformation (C^α RMSD of 0.47 Å) and side chain orientation (C^β RMSD of 0.85 Å).

In the DQ2.5-CLIP1 structure, 14 residues of CLIP1 are clearly visible in the electron density map (**Fig. 3a**). CLIP1 residues MRMATPLLM (Ii 91-99) occupy the P1-P9 pockets of DQ2.5. This binding register is seen in all MHCII-CLIP1 crystal structures solved to date; DR1-CLIP1 (PDB code 3PDO), DR3-CLIP1 (PDB code 1A6A), and I-A^b-CLIP1 (PDB code 1MUJ) (22-24). In the DQ2.5-CLIP2 structure, 12 residues of CLIP2 are clearly visible in the electron density map (**Fig. 3b**). CLIP2 residues PLLMQALPM (Ii 96-104) occupy the P1-P9 pockets of DQ2.5, which is in agreement

with the biochemically determined binding register of CLIP2 (7,8).

CLIP1 makes 12 direct and 4 water-mediated hydrogen bonds with DQ2.5, whereas CLIP2 makes 14 direct and 6 water-mediated hydrogen bonds with DQ2.5 (**Fig. 2**). There are two hydrogen bond interactions which are present in DQ2.5–CLIP1 but missing in DQ2.5–CLIP2; main chain–main chain interaction between the N–H group of CLIP1 P1 (Ii 91M) and C=O group of DQ2.5 $\alpha 52N$ ($N_{P1} - O_{\alpha 52N}$) and side chain–main chain interaction between the $N^{\eta 1}$ group of CLIP1 P2 (Ii 92R) and C=O group of DQ2.5 $\beta 77R$ ($N_{P2R}^{\eta 1} - O_{\beta 77R}$). The first interaction is not possible in DQ2.5–CLIP2 because CLIP2 has a Pro at P1. There are three hydrogen bond interactions which are present in DQ2.5–CLIP2 but missing in DQ2.5–CLIP1 ($O_{P-3} - N_{\beta 88R}^{\eta 2}$, $O_{P5}^{\epsilon 1} - N_{\beta 70R}^{\eta 2}$, $N_{P6} - O_{\beta 62N}^{\delta 1}$). Equivalent interactions are not possible in DQ2.5–CLIP1 because the main chain C=O group of CLIP1 P-3 is rotated away from DQ2.5 $\beta 88$, and because the P5 and P6 residues of CLIP1 are different from those of CLIP2. Overall, the DQ2.5 binding energies for CLIP1 and CLIP2 appear to be similar, as indicated by the experimentally measured dissociation time for DQ2.5–CLIP1 (140 hours) and DQ2.5–CLIP2 (140 hours) in the absence of DM (8).

Structural basis for the CLIP2 preference of DQ2.5 over CLIP1

Four MHCII–CLIP1 complex crystal structures have been reported to date: DQ2.5–CLIP1 (PDB ID: 5KSU), DR1–CLIP1 (PDB ID: 3PDO) (23), DR3–CLIP1 (PDB ID: 1A6A) (22), and I-A^b–CLIP1 (PDB ID: 1MUJ) (24). Among DQ2.5, DR1, DR3, and I-A^b, only DQ2.5 has been observed to bind CLIP2 (7,8). DQ2.5 has two structural features that may explain why only it is able to bind CLIP2. First, the P4 pocket of DQ2.5 is significantly deeper and broader than that of DR1, DR3 and I-A^b due to polymorphism at $\beta 13$, $\beta 26$ and $\beta 78$ (**Fig. 4**). The calculated volume of the P4 pocket in DQ2.5 is 566 Å³, whereas that of DR1, DR3 and I-A^b ranges from 364 Å³ to 417 Å³. In DQ2.5 the P4 pocket lining residues are $\beta 13G$, $\beta 26L$, and $\beta 78V$. In DR1 they are $\beta 13F$, $\beta 26L$, and $\beta 78Y$. In DR3 they are $\beta 13S$, $\beta 26Y$, and $\beta 78Y$. In I-A^b they are $\beta 13G$, $\beta 26Y$, and $\beta 78V$. Therefore, it

is not surprising that CLIP1, which has Ala at P4, binds to all four MHCII proteins whereas CLIP2, which has Met at P4, only binds to DQ2.5. Second, DQ2.5 has a positively charged peptide binding groove (due to $\beta 70R$, $\beta 71K$ and $\beta 77R$) whereas DR1, DR3, and I-A^b have a negative charged peptide binding groove (due to $\beta 57D$, $\beta 66D$, $\alpha 55E$ in DR1/DR3 and $\beta 57D$, $\beta 66E$, $\alpha 55D$ in I-A^b) (**Fig. 5**). CLIP1 is positively charged (due to P-1 Lys and P2 Arg) while CLIP2 does not contain any charged amino acid residues. Because long-range electrostatic interactions between charged amino acids are important for initial protein–protein complex formation (25–29), DQ2.5 is expected to interact more favorably with CLIP2 than with CLIP1. Indeed, previous biochemical studies have shown that CLIP2 binds to DQ2.5 with higher affinity than CLIP1 (IC₅₀ of 6.0 μM vs. 82.5 μM) (19,30). Among all MHCII proteins whose three dimensional structure has been solved, DQ8 is the only other MHCII which associates with CLIP2 and, consistently, DQ8 has a large P4 pocket and a positively charged peptide binding groove similar to DQ2.5 (**Fig. 5**).

Structural basis for the CLIP-rich phenotype of DQ2.5

DQ2.5 expressing cells have an unusually high CLIP content (up to 53%; CLIP1 and CLIP2 combined) (7–9,19). One possible explanation for this is that DQ2.5 binds CLIP with higher affinity compared to other MHCII. However, the available structural data do not support this notion. Number of direct hydrogen bonds formed between CLIP1 (P-1 to P9 only) and DQ2.5, DR1, DR3, and I-A^b are 11, 13, 17 and 13 respectively. Therefore, we propose that the CLIP-rich phenotype of DQ2.5 arises from an impaired interaction between DQ2.5 and the catalytic DM, whose function is to displace the MHC-bound CLIP peptide. Much of the current structural and mechanistic understanding of MHCII–DM interaction is derived from the DR1–HA–DM crystal structure (PDB ID: 4FQX) (31). We investigated whether DQ2.5 has all the structural elements to facilitate the DM interaction that is observed for DR1–DM. To do this, we built a homology model of DQ2.5–CLIP1–DM. We first examined the electrostatic complementarity of the contact surface areas shared by DQ2.5 and DM (**Fig. 6**). According to our model, two regions in

DQ2.5 make direct contact with DM. The first region is located adjacent to the P1 pocket in the α_1 domain and the second region is located near the transmembrane segment in the α_2 domain. DQ2.5 has better charge complementarity to DM than does DR1, and therefore we can rule out surface electrostatic charge distribution as the source of impaired DQ2.5–DM interaction.

Next, we examined whether DQ2.5 is able to undergo the same set of conformational changes that DR1 undergoes upon DM binding. In DR1, $\alpha 51F$ has been identified as a key DM binding residue (32,33). When DR1 binds to DM, the $\alpha 51$ –55 loop of DR1 transforms into an α -helix which causes the side chain of $\alpha 51F$ to move 13 Å from its initial solvent exposed position to the P1 pocket cavity where it forms a hydrophobic cluster with $\alpha 24F$, $\alpha 31I$, $\alpha 32F$, $\alpha 48F$, and $\beta 89F$ (**Fig. 7**) (31). This hydrophobic interaction is thought to stabilize the otherwise vacant and unstable P1 pocket. DQ2.5 contains a deletion mutation at $\alpha 53$. DM sensitivity of DQ2.5 was found to be partially restored upon insertion of a Gly at this position (34). Because of the deletion of at $\alpha 53$ in DQ2.5, $\alpha 51F$ is located at a position that is inaccessible by DM. This unconventional location of $\alpha 51F$ may compromise the DQ2.5–DM interaction. Further, we suggest that the DM insensitivity of DQ2.5 is due to the presence of an extensive hydrogen bond network (involving $\alpha 9Y$, $\alpha 22Y$, $\alpha 24H$, $\alpha 31Q$, $\beta 86E$, $\beta 90T$, and a buried water molecule) that spans the P1 to the P4 pockets of DQ2.5 (**Fig. 8a**). We carried out a 50ns molecular dynamics (MD) simulation of the DQ2.5–CLIP1 complex to assess the stability of this hydrogen bond network. MD trajectories show that all hydrogen bonds in this network, with the exception of the peripheral $\beta 86E$ O^{ε1}– $\beta 90T$ O^γ, are stable (**Fig. 9**). Furthermore, we observed that $\alpha 51F$ does not enter the P1 pocket during the course of the DQ2.5–CLIP1–DM MD simulation, likely due to the presence of the $\alpha 9$ – $\alpha 22$ – $\alpha 24$ – $\alpha 31$ – $\beta 86$ – $\beta 90$ hydrogen bond network (**Fig. 10a**). In particular, the water molecule which is hydrogen bonded to $\alpha 24H$ and $\alpha 31Q$ is directly blocking the P1 pocket. We mutated the $\alpha 24$, $\alpha 31$, and $\beta 86$ residues in our DQ2.5–CLIP1–DM model to their counterpart in DR1; E $\beta 86G$, Q $\alpha 31I$ and H $\alpha 24F$. These mutations are expected to disrupt the $\alpha 9$ – $\alpha 22$ – $\alpha 24$ – $\alpha 31$ – $\beta 86$ – $\beta 90$ hydrogen bond network, and potentially fully restore DM

sensitivity in DQ2.5. Our 50 ns MD simulation of the triple mutant DQ2.5 shows that $\alpha 51F$ does indeed occupy the P1 pocket (**Fig. 10b**), as seen in the DR1–HA–DM crystal structure (**Fig. 10c**, **Fig. 11**). In DR1, DM binding also causes the $\beta 85$ –90 region to change from an α -helix to a loop, which causes $\beta 89F$ to move 4.7 Å from the protein surface to the P1 pocket floor where it forms a hydrophobic cluster with several other hydrophobic residues including $\alpha 51F$ (31) (**Fig. 7b**). In DQ2.5, similar rearrangement of the $\beta 85$ –90 region does not appear feasible as $\beta 86E$ and $\beta 90T$ are held in place by the $\alpha 9$ – $\alpha 22$ – $\alpha 24$ – $\alpha 31$ – $\beta 86$ – $\beta 90$ hydrogen bond network (**Fig. 8a**). In summary, the $\alpha 9$ – $\alpha 22$ – $\alpha 24$ – $\alpha 31$ – $\beta 86$ – $\beta 90$ hydrogen bond network in DQ2.5 prevents repositioning of $\alpha 51F$ and $\beta 89F$, which is important in DR1–DM interaction.

Hydrogen bond between the P1 main chain nitrogen of CLIP1 and the $\alpha 52$ carbonyl group of DQ2.5

All crystal structures of MHCII in complex with a peptide whose P1 residue is not Pro have a hydrogen bond between the amide nitrogen of the P1 residue and the main chain carbonyl group of MHCII $\alpha 53$. Interestingly, DQ2.5 has a deletion mutation at $\alpha 53$, and as gluten peptides binding to DQ2.5 frequently have Pro at P1, it was suggested that DQ2.5 is unable to form this hydrogen bond (34). The significance of this peptide main chain hydrogen bond has been assessed by comparing binding of peptides being N-methylated at the P1 position with unmodified peptides. Whereas such substitution gave decreased affinity for peptide binding to DR1 no effect was seen for DQ2.5 (35,36). Interestingly, our DQ2.5–CLIP1 structure shows that there is indeed a hydrogen bond between the P1 main chain nitrogen of CLIP1 and the $\alpha 52$ carbonyl group of DQ2.5. The gluten derived DQ2.5-glia- $\alpha 1a$ T-cell epitope (LQPF^QPELPY, underlined residue is P1) binds to DQ2.5 with two-fold higher affinity than the analog peptide containing norvaline (Nva) at P1 (~25 μ M) (37). Nva is a non-proteinogenic alpha amino acid which is isosteric to Pro but has a primary amine group which is able to participate in hydrogen bonding. Therefore, DQ2.5-glia- $\alpha 1a$ must have an overall energetic advantage over the Nva substituted analog peptide for binding to DQ2.5, despite having a hydrogen

bond deficiency at P1. We propose that DQ2.5-glia- α 1a, as well as other peptides containing Pro at P1, have an entropic advantage that compensates for the lost enthalpy associated with the P1 hydrogen bond.

Discussion

We have determined the crystal structure of DQ2.5-CLIP1 (PDB ID: 5KSU) and DQ2.5-CLIP2 (PDB ID: 5KSV), at 2.73 Å and 2.20 Å respectively. While crystal structure of CLIP1 in complex with DR1 (with the peptide bound in both forward and reverse directions) (23,38), DR3 (22), and I-A^b (24) has been reported previously, no crystal structure of CLIP2 bound to an MHCII has been reported so far. DQ2.5 is unusual in that it associates with CLIP1 (Ii 83-101) as well as the non-canonical CLIP2 (Ii 92-107) (19). Our study has revealed two unique structural features of DQ2.5 that may promote its association with CLIP2. First, DQ2.5 has an unusually large P4 pocket which can accommodate the bulky P4 Met of CLIP2. Second, DQ2.5 has a positively charged peptide binding groove, which is electrostatically more compatible with the neutral CLIP2 compared to the positively charged CLIP1.

Another unusual characteristic of DQ2.5 is its CLIP-rich phenotype. CLIP1 and CLIP2 combined account for 53% of the eluted peptide pool (9). It was proposed that the CLIP-rich phenotype of DQ2.5 is explained by MHCII-CLIP being poor substrates for HLA-DM (8,21). During MHC maturation, DM catalyzes release of CLIP from the nascent MHC (5). Therefore, impaired DQ2.5-DM interaction will result in DQ2.5 molecules retaining their original CLIP cargo. In contrast, DR1 expressing cells have low abundance of CLIP (20), which suggests that DR1 is a good substrate for DM. We found two structural elements in DQ2.5 that may lower its DM sensitivity. First, α 51, which is a key DM contacting residue in DR1, is positioned internally in DQ2.5 due to the α 53 deletion mutation. Second, the peptide binding groove residues which form the α 9- α 22- α 24- α 31- β 86- β 90 hydrogen bond network are not as free to move about as the corresponding residues in DR1 (Fig. 8). Therefore, DQ2.5 is less predisposed to the drastic secondary structure changes that DR1 undergoes upon DM

binding. Our MD study showed that the α 9- α 22- α 24- α 31- β 86- β 90 hydrogen bond network is stable and also that α 51F of DQ2.5 cannot move into the P1 pocket upon DM binding. This is due to the blockage of the P1 pocket entrance by a water molecule which is part of the α 9- α 22- α 24- α 31- β 86- β 90 hydrogen bond network. To further test this idea, we disrupted the hydrogen bond network by changing α 24, α 31 and β 86 to the hydrogen bond non-permissible residues and then repeated the MD exercise. This time, α 51F did translocate to fill the P1 pocket, similar to what happens in DR1 upon DM binding. Our hypothesis that the α 9- α 22- α 24- α 31- β 86- β 90 hydrogen bond network leads to diminished DM sensitivity and ultimately to the CLIP-rich phenotype is further supported by a recent study by Zhou and colleagues who showed that changing β 86 of DQ8 from Glu to Ala resulted in increased DM sensitivity (21). DQ8 has the same α 9- α 22- α 24- α 31- β 86- β 90 hydrogen bond network found in DQ2.5, although it does not have the α 53 deletion mutation. Our analysis, however, is based on the assumption that the DR1-DM interaction mechanism is directly applicable to DQ2.5-DM. It remains to be seen if the DR1-DM interaction mechanism is truly universal. Even if this should prove not to be the case, the preference of bulky hydrophobic anchor residues at the P1 pocket for both DR1 (39,40) and DQ2.5 (19,30) indicates that these two molecules likely share the mechanistic feature of α 51F translocating to fill the P1 pocket in the interaction with DM.

There are two other human MHCII alleles which have a deletion mutation at α 53 like DQ2.5 and also contain the same set of residues that make up the α 9- α 22- α 24- α 31- β 86- β 90 hydrogen bond network in DQ2.5; DQ4.4 (DQA1*04:01/DQB1*04:02) and DQ7.5 (DQA1*05:05/DQB1*03:01) (14). We predict DQ4.4 and DQ7.5 to be poor substrates for DM and to have a CLIP-rich phenotype, similar to DQ2.5. Interestingly, DQ2.5, DQ4.4, and DQ7.5 are all associated with one or more human autoimmune disorders. DQ2.5 is associated with celiac disease and type 1 diabetes, DQ4.4 is associated with juvenile idiopathic arthritis (41), and DQ7.5 is associated with celiac disease (9,42). However, there is no known mechanistic link

between decreased DM sensitivity and human autoimmune disorders.

Experimental procedures

Expression and Purification

DQ2.5 (DQA1*05:01/DQB1*02:01) containing covalently linked CLIP1 and CLIP2 were prepared in a manner similar to DQ2.5- α I gliadin (15,43-45). Fos and Jun leucine zipper sequences were attached to the C-terminus of the α and β chains, respectively, through intervening Factor Xa sites to promote heterodimer stability. The CLIP1 (PVSKMRMATPLLMQA) and CLIP2 (MATPLLMQALPMGAL) peptides were attached to the N terminus of the β chain using a 15 residue linker. Expression of DQ2.5 molecules was done as detailed elsewhere (43) using baculovirus, ExpresSF+ insect cells and the mAb 2.12.E11 (46) for affinity purification.

Crystallization and data collection

DQ2.5-CLIP1 and DQ2.5-CLIP2 were treated with Factor Xa for 16 hours at 24°C to remove the leucine zippers from the MHCII. MHCII was then purified using anion exchange (buffer A: 25 mM Tris, pH 8.0, buffer B: 25 mM Tris, pH 8.0, 0.5 M NaCl) and size exclusion chromatography (buffer: 25 mM Tris, pH 8.0) and concentrated to 2 mg/ml. For DQ2.5-CLIP1, 1 μ l of the protein solution and 1 μ l of precipitant buffer (0.1 M ammonium sulphate, 0.1 M sodium cacodylate, pH 6.5, 25% PEG 8000 and 6% glycerol) were combined in a single hanging drop and kept at 18°C. For DQ2.5-CLIP2, 1 μ l of the protein solution and 1 μ l of precipitant buffer (0.1 M BIS-TRIS, pH 5.5, 22% PEG 3350) was combined in a single hanging drop and kept at 18°C. Small crystals of DQ2.5-CLIP1 and DQ2.5-CLIP2 appeared within one week and grew to full size in two weeks. Crystals were soaked in mother liquor containing 5% glycerol and then flash frozen in liquid nitrogen. X-ray diffraction data were collected at beam line 9-3 of the Stanford Synchrotron Radiation Laboratory. Diffraction data indexing and integrating was done using HKL2000 (47). DQ2.5-CLIP1 crystal belonged to the C121 space group with cell dimensions a=128.86 b=69.21 c=146.69. DQ2.5-CLIP2

crystal belonged to the I23 space group with cell dimensions a=137.01 b=137.01 c=137.01.

Structure determination and analysis

Both structures were determined by molecular replacement using Phaser (48,49). DQ2.5 coordinates from the DQ2.5-gliadin structure (PDB ID: 1S9V) was used as the search model. Model refinement was carried out using Refmac (50), Phenix (51), and Coot (49). CLIP1 and CLIP2 peptides were built at the end of refinement, guided by the F_o-F_c electron density map. Bulk solvent correction and isotropic B correction were applied throughout the refinement. Water molecules were identified from residual density greater than 1.0σ in the $2F_o-F_c$ map. All water molecules were checked for valid geometry, environment, and density shape before conducting additional cycles of model building and refinement. Two last refinement rounds included TLS (translation, libration, and screw-rotation displacements) parameterization. Crystallographic data collection, processing, and refinement statistics are given in Table 1. The stereochemical quality of the final structures were carried out using PROCHECK (52).

Model building of DQ2.5(wild type)-CLIP1-DM and DQ2.5(E β 86G, Q α 31I, H α 24F)-CLIP1-DM

The wild type and mutant DQ2.5-CLIP1-DM complex were modeled using the MODELLER v9.10 suite of programs (53). The DR1-HA-DM (PDB code: 4FQX) and DQ2.5-CLIP1 (PDB ID: 5KSU) crystal structures were used as templates. In this model, CLIP1 was truncated to the same length (from P2 to P10) as that of the HA peptide in the DR1-HA-DM crystal structure. Total of 5 models were created and evaluated using the DOPE statistical energy function (54). Slow refine option was applied to achieve energy minimized models. Structure visualization and figure representation were done using Chimera (55) and Pymol (56).

Molecular dynamics simulations

All-atom molecular dynamics (MD) simulation was carried out on three systems: DQ2.5(wild type)-CLIP1, DQ2.5(wild type)-CLIP1-DM and DQ2.5(E β 86G, Q α 31I, H α 24F)-CLIP1-DM. All crystal water molecules were included in the starting MD structures given their

importance in mediating the protein–peptide interaction (57-59). Standard protonation state, at pH 7.0, is applied for all ionizable amino acid groups, i.e. Lys and Arg side chains are protonated, while Glu and Asp side chains are deprotonated. His side chains, by default, are singly protonated. Each system was solvated with TIP3P water box with the minimum distance of 12 Å to any protein atom and neutralized by sodium counter ions. Periodic boundary conditions were applied on the system.

The complex was first energy minimized using steepest descent and conjugate gradient minimization, followed by heating to 300K within 800 ps under NVT conditions. The system was then equilibrated under NPT conditions within 1 ns. The MD simulations under NVE conditions were carried out for 50 ns.

Acknowledgements

This work was supported by the STARs Program of University of Texas System and institutional funding from The University of Texas at El Paso awarded to Chu-Young Kim. Thanh-Binh Nguyen is a recipient of the SINGA scholarship from the Agency for Science, Technology and Research, Singapore. Mallur S. Madhusudhan is supported by a senior fellowship of the Wellcome Trust/DBT India alliance. The work in the laboratory of Ludvig M. Sollid was supported by the Research Council of Norway through its Centres of Excellence funding scheme, project number 179573/V40 as well as by the South-Eastern Norway Regional Health Authority. Data collection was performed at the Stanford Synchrotron Radiation Lightsource, SLAC National Accelerator Laboratory, which is supported by the U.S. Department of Energy, Office of Science, Office of Basic Energy Sciences under Contract No. DE-AC02-76SF00515. The SSRL Structural Molecular Biology Program is supported by the DOE Office of Biological and Environmental Research, and by the National Institutes of Health, National Institute of General Medical Sciences (including P41GM103393). We thank Dr. I. I. Mathews at SSRL for assistance with X-ray data collection and processing, and Dr. Chandra Verma at Bioinformatics Institute for discussion on molecular dynamics simulation.

Author Contributions

CK and LMS conceived and coordinated the study. CK, TN, and LMS wrote the paper. EB carried out recombinant protein expression and purification. TN and PJ conducted X-ray crystallography experiments. TN and MSM conducted molecular dynamics simulation experiments. All authors reviewed the results and approved the final version of the manuscript.

Conflict of Interest

The authors declare that they have no conflicts of interest with the contents of this article.

SHAKE was turned on for all bonds involving hydrogen. All simulations were carried out with the AMBER12 program (60) together with the ff99SB (61) force fields. The Particle Mesh Ewald (PME) (62) algorithm was used to calculate long range interactions while short range interactions were truncated at 10.0 Å. The integration time step was set to 1 fs. Resulting trajectories were analyzed using a combination of indigenously developed Python scripts and the Ptraj/Cpptraj module of Amber12.

Pocket volume calculation

Volume of the P4 pocket in DQ2.5, DR1, DR3, and I-A^b was calculated using an in-house script based on the Voronoi algorithm (63).

References

1. Cresswell, P. (1994) Assembly, transport, and function of MHC class II molecules. *Annu. Rev. Immunol.* **12**, 259-293
2. Roche, P. A., Marks, M. S., and Cresswell, P. (1991) Formation of a nine-subunit complex by HLA class II glycoproteins and the invariant chain. *Nature* **354**, 392-394
3. Brodsky, F. M., and Guagliardi, L. E. (1991) The cell biology of antigen processing and presentation. *Annu. Rev. Immunol.* **9**, 707-744
4. Riberdy, J. M., Newcomb, J. R., Surman, M. J., Barbosa, J. A., and Cresswell, P. (1992) HLA-DR molecules from an antigen-processing mutant cell line are associated with invariant chain peptides. *Nature* **360**, 474-477
5. Sette, A., Southwood, S., Miller, J., and Appella, E. (1995) Binding of major histocompatibility complex class II to the invariant chain-derived peptide, CLIP, is regulated by allelic polymorphism in class II. *J. Exp. Med.* **181**, 677-683
6. Sloan, V. S., Cameron, P., Porter, G., Gammon, M., Amaya, M., Mellins, E., and Zaller, D. M. (1995) Mediation by HLA-DM of dissociation of peptides from HLA-DR. *Nature* **375**, 802-806
7. Wiesner, M., Stepniak, D., de Ru, A. H., Moustakis, A. K., Drijfhout, J. W., Papadopoulos, G. K., van Veelen, P. A., and Koning, F. (2008) Dominance of an alternative CLIP sequence in the celiac disease associated HLA-DQ2 molecule. *Immunogenetics* **60**, 551-555
8. Fallang, L. E., Roh, S., Holm, A., Bergseng, E., Yoon, T., Fleckenstein, B., Bandyopadhyay, A., Mellins, E. D., and Sollid, L. M. (2008) Complexes of two cohorts of CLIP peptides and HLA-DQ2 of the autoimmune DR3-DQ2 haplotype are poor substrates for HLA-DM. *J. Immunol.* **181**, 5451-5461
9. Bergseng, E., Dorum, S., Arntzen, M. O., Nielsen, M., Nygard, S., Buus, S., de Souza, G. A., and Sollid, L. M. (2015) Different binding motifs of the celiac disease-associated HLA molecules DQ2.5, DQ2.2, and DQ7.5 revealed by relative quantitative proteomics of endogenous peptide repertoires. *Immunogenetics* **67**, 73-84
10. Karell, K., Louka, A. S., Moodie, S. J., Ascher, H., Clot, F., Greco, L., Ciclitira, P. J., Sollid, L. M., and Partanen, J. (2003) HLA types in celiac disease patients not carrying the DQA1*05-DQB1*02 (DQ2) heterodimer: results from the European Genetics Cluster on Celiac Disease. *Hum Immunol* **64**, 469-477
11. Sollid, L. M., Markussen, G., Ek, J., Gjerde, H., Vartdal, F., and Thorsby, E. (1989) Evidence for a primary association of celiac disease to a particular HLA-DQ alpha/beta heterodimer. *J. Exp. Med.* **169**, 345-350
12. Todd, J. A., Bell, J. I., and McDevitt, H. O. (1987) HLA-DQ beta gene contributes to susceptibility and resistance to insulin-dependent diabetes mellitus. *Nature* **329**, 599-604
13. Trier, J. S. (1991) Celiac Sprue. *New Engl. J. Med.* **325**, 1709-1719
14. Karell, K., Louka, A. S., Moodie, S. J., Ascher, H., Clot, F., Greco, L., Ciclitira, P. J., Sollid, L. M., and Partanen, J. (2003) HLA types in celiac disease patients not carrying the DQA1*05-DQB1*02 (DQ2) heterodimer: results from the European Genetics Cluster on Celiac Disease. *Hum. Immunol.* **64**, 469-477
15. Kim, C. Y., Quarsten, H., Bergseng, E., Khosla, C., and Sollid, L. M. (2004) Structural basis for HLA-DQ2-mediated presentation of gluten epitopes in celiac disease. *Proc. Natl. Acad. Sci. USA* **101**, 4175-4179
16. Petersen, J., Montserrat, V., Mujico, J. R., Loh, K. L., Beringer, D. X., van Lummel, M., Thompson, A., Mearin, M. L., Schweizer, J., Kooy-Winkelaar, Y., van Bergen, J., Drijfhout, J. W., Kan, W. T., La Gruta, N. L., Anderson, R. P., Reid, H. H., Koning, F., and Rossjohn, J. (2014) T-cell receptor recognition of HLA-DQ2-gliadin complexes associated with celiac disease. *Nat. Struct. Mol. Biol.* **21**, 480-488

17. Stepniak, D., Wiesner, M., de Ru, A. H., Moustakas, A. K., Drijfhout, J. W., Papadopoulos, G. K., van Veelen, P. A., and Koning, F. (2008) Large-scale characterization of natural ligands explains the unique gluten-binding properties of HLA-DQ2. *J. Immunol.* **180**, 3268-3278
18. Busch, R., De Riva, A., Hadjinicolaou, A. V., Jiang, W., Hou, T., and Mellins, E. D. (2012) On the perils of poor editing: regulation of peptide loading by HLA-DQ and H2-A molecules associated with celiac disease and type 1 diabetes. *Expert Rev. Mol. Med.* **14**, e15
19. Vartdal, F., Johansen, B. H., Friede, T., Thorpe, C. J., Stevanović, S., Eriksen, J. E., Sletten, K., Thorsby, E., Rammensee, H.-G., and Sollid, L. M. (1996) The peptide binding motif of the disease associated HLA-DQ (α 1* 0501, β 1* 0201) molecule. *Eur. J. Immunol.* **26**, 2764-2772
20. Chicz, R. M., Urban, R. G., Lane, W. S., Gorga, J. C., Stern, L. J., Vignali, D. A., and Strominger, J. L. (1992) Predominant naturally processed peptides bound to HLA-DR1 are derived from MHC-related molecules and are heterogeneous in size. *Nature* **358**, 764-768
21. Zhou, Z., Reyes-Vargas, E., Escobar, H., Rudd, B., Rockwood, A. L., Delgado, J. C., He, X., and Jensen, P. E. (2015) Type 1 diabetes associated HLA-DQ2 and DQ8 molecules are relatively resistant to HLA-DM mediated release of invariant chain-derived CLIP peptides. *Eur. J. Immunol.*
22. Ghosh, P., Amaya, M., Mellins, E., and Wiley, D. C. (1995) The structure of an intermediate in class II MHC maturation: CLIP bound to HLA-DR3. *Nature* **378**, 457-462
23. Gunther, S., Schlundt, A., Sticht, J., Roske, Y., Heinemann, U., Wiesmuller, K. H., Jung, G., Falk, K., Rotzschke, O., and Freund, C. (2010) Bidirectional binding of invariant chain peptides to an MHC class II molecule. *Proc. Natl. Acad. Sci. USA* **107**, 22219-22224
24. Zhu, Y., Rudensky, A. Y., Corper, A. L., Teyton, L., and Wilson, I. A. (2003) Crystal structure of MHC class II I-Ab in complex with a human CLIP peptide: prediction of an I-Ab peptide-binding motif. *J. Mol. Biol.* **326**, 1157-1174
25. Camacho, C. J., Weng, Z., Vajda, S., and DeLisi, C. (1999) Free energy landscapes of encounter complexes in protein-protein association. *Biophys. J.* **76**, 1166-1178
26. Drozdov-Tikhomirov, L. N., Linde, D. M., Poroikov, V. V., Alexandrov, A. A., and Skurida, G. I. (2001) Molecular mechanisms of protein-protein recognition: whether the surface placed charged residues determine the recognition process? *J. Biomol. Struct. Dyn.* **19**, 279-284
27. Chu, X., Wang, Y., Gan, L., Bai, Y., Han, W., Wang, E., and Wang, J. (2012) Importance of electrostatic interactions in the association of intrinsically disordered histone chaperone Chz1 and histone H2A.Z-H2B. *PLoS Comp. Biol.* **8**, e1002608
28. Kumar, V., Dixit, N., Zhou, L. L., and Fraunhofer, W. (2011) Impact of short range hydrophobic interactions and long range electrostatic forces on the aggregation kinetics of a monoclonal antibody and a dual-variable domain immunoglobulin at low and high concentrations. *Int. J. Pharm.* **421**, 82-93
29. Uchikoga, N., Takahashi, S. Y., Ke, R., Sonoyama, M., and Mitaku, S. (2005) Electric charge balance mechanism of extended soluble proteins. *Protein Sci.* **14**, 74-80
30. Wal, Y., Kooy, Y. C., Drijfhout, J., Amons, R., and Koning, F. (1996) Peptide binding characteristics of the coeliac disease-associated DQ(α 1*0501, β 1*0201) molecule. *Immunogenetics* **44**, 246-253
31. Pos, W., Sethi, D. K., Call, M. J., Schulze, M. S., Anders, A. K., Pyrdol, J., and Wuchterpfennig, K. W. (2012) Crystal structure of the HLA-DM-HLA-DR1 complex defines mechanisms for rapid peptide selection. *Cell* **151**, 1557-1568
32. Doebele, R. C., Busch, R., Scott, H. M., Pashine, A., and Mellins, E. D. (2000) Determination of the HLA-DM interaction site on HLA-DR molecules. *Immunity* **13**, 517-527
33. Painter, C. A., Negroni, M. P., Kellersberger, K. A., Zavala-Ruiz, Z., Evans, J. E., and Stern, L. J. (2011) Conformational lability in the class II MHC 310 helix and adjacent extended strand dictate HLA-DM susceptibility and peptide exchange. *Proc. Natl. Acad. Sci. USA* **108**, 19329-19334

34. Hou, T., Macmillan, H., Chen, Z., Keech, C. L., Jin, X., Sidney, J., Strohma, M., Yoon, T., and Mellins, E. D. (2011) An insertion mutant in DQA1*0501 restores susceptibility to HLA-DM: implications for disease associations. *J. Immunol.* **187**, 2442-2452
35. Stratikos, E., Wiley, D. C., and Stern, L. J. (2004) Enhanced catalytic action of HLA-DM on the exchange of peptides lacking backbone hydrogen bonds between their N-terminal region and the MHC class II alpha-chain. *J. Immunol.* **172**, 1109-1117
36. Yin, L., Trenh, P., Guce, A., Wiczorek, M., Lange, S., Sticht, J., Jiang, W., Bylsma, M., Mellins, E. D., Freund, C., and Stern, L. J. (2014) Susceptibility to HLA-DM protein is determined by a dynamic conformation of major histocompatibility complex class II molecule bound with peptide. *J. Biol. Chem.* **289**, 23449-23464
37. Bergseng, E., Xia, J., Kim, C. Y., Khosla, C., and Sollid, L. M. (2005) Main chain hydrogen bond interactions in the binding of proline-rich gluten peptides to the celiac disease-associated HLA-DQ2 molecule. *J. Biol. Chem.* **280**, 21791-21796
38. Schlundt, A., Gunther, S., Sticht, J., Wiczorek, M., Roske, Y., Heinemann, U., and Freund, C. (2012) Peptide linkage to the alpha-subunit of MHCII creates a stably inverted antigen presentation complex. *J Mol Biol* **423**, 294-302
39. Jardetzky, T. S., Gorga, J. C., Busch, R., Rothbard, J., Strominger, J. L., and Wiley, D. C. (1990) Peptide binding to HLA-DR1: a peptide with most residues substituted to alanine retains MHC binding. *EMBO J.* **9**, 1797-1803
40. Falk, K., Rotzschke, O., Stevanovic, S., Jung, G., and Rammensee, H. G. (1994) Pool sequencing of natural HLA-DR, DQ, and DP ligands reveals detailed peptide motifs, constraints of processing, and general rules. *Immunogenetics* **39**, 230-242
41. Volz, T., Schwarz, G., Fleckenstein, B., Schepp, C. P., Haug, M., Roth, J., Wiesmuller, K. H., and Dannecker, G. E. (2004) Determination of the peptide binding motif and high-affinity ligands for HLA-DQ4 using synthetic peptide libraries. *Hum. Immunol.* **65**, 594-601
42. Tinto, N., Cola, A., Piscopo, C., Capuano, M., Galatola, M., Greco, L., and Sacchetti, L. (2015) High Frequency of Haplotype HLA-DQ7 in Celiac Disease Patients from South Italy: Retrospective Evaluation of 5,535 Subjects at Risk of Celiac Disease. *PLoS One* **10**, e0138324
43. Quarsten, H., McAdam, S. N., Jensen, T., Arentz-Hansen, H., Molberg, O., Lundin, K. E., and Sollid, L. M. (2001) Staining of celiac disease-relevant T cells by peptide-DQ2 multimers. *J. Immunol.* **167**, 4861-4868
44. Kozono, H., White, J., Clements, J., Marrack, P., and Kappler, J. (1994) Production of soluble MHC class II proteins with covalently bound single peptides. *Nature* **369**, 151-154
45. Kalandadze, A., Galleno, M., Foncerrada, L., Strominger, J. L., and Wucherpennig, K. W. (1996) Expression of recombinant HLA-DR2 molecules. Replacement of the hydrophobic transmembrane region by a leucine zipper dimerization motif allows the assembly and secretion of soluble DR alpha beta heterodimers. *J Biol Chem* **271**, 20156-20162
46. Viken, H. D., Paulsen, G., Sollid, L. M., Lundin, K. E., Tjonnfjord, G. E., Thorsby, E., and Gaudernack, G. (1995) Characterization of an HLA-DQ2-specific monoclonal antibody. Influence of amino acid substitutions in DQ beta 1*0202. *Hum. Immunol.* **42**, 319-327
47. Otwinowski, Z., and Minor, W. (1997) Processing of X-ray diffraction data collected in oscillation mode. Elsevier. pp 307-326
48. McCoy, A. J., Grosse-Kunstleve, R. W., Adams, P. D., Winn, M. D., Storoni, L. C., and Read, R. J. (2007) Phaser crystallographic software. *Journal of Applied Crystallography* **40**, 658-674
49. Emsley, P., Lohkamp, B., Scott, W. G., and Cowtan, K. (2010) Features and development of Coot. *Acta Crystallographica Section D* **66**, 486-501
50. Murshudov, G. N., Vagin, A. A., and Dodson, E. J. (1997) Refinement of Macromolecular Structures by the Maximum-Likelihood Method. *Acta Crystallographica Section D* **53**, 240-255
51. Adams, P. D., Afonine, P. V., Bunkoczi, G., Chen, V. B., Davis, I. W., Echols, N., Headd, J. J., Hung, L. W., Kapral, G. J., Grosse-Kunstleve, R. W., McCoy, A. J., Moriarty, N. W., Oeffner, R., Read, R. J., Richardson, D. C., Richardson, J. S., Terwilliger, T. C., and Zwart, P. H. (2010)

- PHENIX: a comprehensive Python-based system for macromolecular structure solution. *Acta Crystallogr D Biol Crystallogr* **66**, 213-221
52. Laskowski, R. A., MacArthur, M. W., Moss, D. S., and Thornton, J. M. (1993) PROCHECK: a program to check the stereochemical quality of protein structures. *Journal of Applied Crystallography* **26**, 283-291
 53. Eswar, N., Webb, B., Marti-Renom, M. A., Madhusudhan, M. S., Eramian, D., Shen, M. Y., Pieper, U., and Sali, A. (2007) Comparative protein structure modeling using MODELLER. *Curr. Protoc. Protein Sci.* **Chapter 2**, Unit 2 9
 54. Shen, M. Y., and Sali, A. (2006) Statistical potential for assessment and prediction of protein structures. *Protein Sci* **15**, 2507-2524
 55. Pettersen, E. F., Goddard, T. D., Huang, C. C., Couch, G. S., Greenblatt, D. M., Meng, E. C., and Ferrin, T. E. (2004) UCSF Chimera--a visualization system for exploratory research and analysis. *J Comput Chem* **25**, 1605-1612
 56. Schrodinger, LLC. (2014) The PyMOL Molecular Graphics System, Version 1.7.
 57. Li, Y., Yang, Y., He, P., and Yang, Q. (2009) QM/MM study of epitope peptides binding to HLA-A*0201: the roles of anchor residues and water. *Chem Biol Drug Des* **74**, 611-618
 58. Petrone, P. M., and Garcia, A. E. (2004) MHC-peptide binding is assisted by bound water molecules. *J Mol Biol* **338**, 419-435
 59. Ogata, K., and Wodak, S. J. (2002) Conserved water molecules in MHC class-I molecules and their putative structural and functional roles. *Protein Eng* **15**, 697-705
 60. Case, D. A., Darden, T. A., Cheatham, T. E., Simmerling, C. L., Wang, J., Duke, R. E., Luo, R., Walker, R. C., Zhang, W., Merz, K. M., Roberts, B., Hayik, S., Roitberg, A., Seabra, G., Swails, J., Goetz, A. W., Kolossváry, I., Wong, K. F., Paesani, F., Vanicek, J., Wolf, R. M., Liu, J., Wu, X., Brozell, S. R., Steinbrecher, T., Gohlke, H., Cai, Q., Ye, X., Hsieh, M. J., Cui, G., Roe, D. R., Mathews, D. H., Seetin, M. G., Salomon-Ferrer, R., Sagui, C., Babin, V., Luchko, T., Gusarov, S., Kovalenko, A., and Kollman, P. A. (2012) AMBER 12. University of California, San Francisco
 61. Hornak, V., Abel, R., Okur, A., Strockbine, B., Roitberg, A., and Simmerling, C. (2006) Comparison of multiple Amber force fields and development of improved protein backbone parameters. *Proteins* **65**, 712-725
 62. Darden, T., York, D., and Pedersen, L. (1993) Particle mesh Ewald: An N·log(N) method for Ewald sums in large systems. *J. Chem. Phys.* **98**, 10089-10092
 63. Richards, F. M. (1974) The interpretation of protein structures: total volume, group volume distributions and packing density. *J. Mol. Biol.* **82**, 1-14

Figure legends

Figure 1. (a) Amino acid sequence of the human invariant chain protein. MHCII binding core sequence of CLIP1 is MRMATPLLM and that of CLIP2 is PLLMQALPM. MHCII binding core sequence of CLIP3 is unknown. (b) Solution NMR structure of the truncated human invariant chain protein (residues 118-192, PDB ID: 1IIE). The invariant chain protein is a homo-trimer and associates with three class II major histocompatibility complex proteins simultaneously in the endoplasmic reticulum.

Figure 2. (a) Crystal structure of DQ2.5–CLIP1 (PDB ID: 5KSU). (b) Crystal structure of HLA-DQ2.5–CLIP2 (PDB ID: 5KSV). DQ2.5 α -chain and β -chain are shown in blue and pink, respectively. CLIP1 and CLIP2 peptides are drawn as a stick model (light yellow, carbon; dark yellow, sulfur; blue, nitrogen; red, oxygen). Hydrogen bond interactions are shown as red broken lines.

Figure 3. 2Fo-Fc electron density map of (a) CLIP1 and (b) CLIP2, both contoured at 1.0 σ . CLIP1 and CLIP2 peptides are shown in stick representation (light yellow, carbon; dark yellow, sulfur; blue, nitrogen; red, oxygen).

Figure 4. Close up view of the P4 pocket in (a) DQ2.5–CLIP1 (PDB ID: 5KSU), (b) DR1–CLIP1 (PDB ID: 3PDO), (c) DR3–CLIP1 (PDB ID: 1A6A), and (d) I-A^b–CLIP1 (PDB ID: 1MUJ). The protein surface of the MHCII α -chain and β -chain are colored blue and pink, respectively. β -chain residues that line the P4 pocket are shown as a stick model (pink, carbon; red, oxygen). CLIP1 peptide is shown in yellow.

Figure 5. Adaptive Poisson Boltzmann Solver (APBS)-generated electrostatic surface of MHC class II proteins at pH 7.0 (red = negative, blue = positive, white = neutral). The view is from the top, looking straight into the peptide binding groove. (a) DQ2.5–CLIP1 (PDB ID: 5KSU), (b) DR1–CLIP1 (PDB ID: 3PDO), (c) DR3–CLIP1 (PDB ID: 1A6A), (d) I-A^b–CLIP1 (PDB ID: 1MUJ), (e) DR2w2a–Epstein Barr Virus DNA polymerase peptide (PDB ID: 1H15), (f) DR4w4–human collagen II peptide (PDB ID: 2SEB), (g) DR52a–integrin beta 3 peptide (PDB ID: 2Q6W), (h) DQ8–deamidated gluten peptide (PDB ID: 2NNA), (i) I-A^d–influenza hemagglutinin peptide (PDB ID: 2IAD), (j) I-A^g–hel 11-27 peptide (PDB ID: 3MBE), (k) I-A^k–conalbumin peptide (PDB ID: 1D9K), and (l) I-E^k–MCC peptide (PDB ID: 3QIU). MHC bound peptides were not included in the APBS electrostatics calculations.

Figure 6. The regions of contact shared by MHCII and HLA-DM are indicated as corresponding ovals. The protein surface color represents Adaptive Poisson Boltzmann Solver-generated electrostatics surface of MHC class II proteins at pH 5.5 (red = negative, blue = positive, white = neutral). (a) DQ2.5 from DQ2.5–CLIP1 (PDB ID: 5KSU), (b) DR1 from DR1–HA–DM (PDB ID: 4FQX) and (c) DM from DR1–HA–DM (PDB ID: 4FQX).

Figure 7. Conformation of the peptide binding groove in (a) DQ2.5–CLIP1 (PDB ID: 5KSU), (b) DR1–CLIP1 (PDB ID: 3PDO) and (c) DR1–HA–DM (PDB ID: 4FQX). α -chain and β -chain of the MHCII are colored in blue and pink respectively. The MHCII bound peptide is omitted for clarity.

Figure 8. Hydrogen bond network found at the bottom of the MHCII peptide binding groove. (a) DQ2.5–CLIP1 (PDB ID: 5KSU), (b) DR1–CLIP1 (PDB ID: 3PDO), (c) DR3–CLIP1 (PDB ID: 1A6A), and (d) I-A^b–CLIP1 (PDB ID: 1MUJ). MHCII α -chain and β -chain are shown in blue and pink, respectively. MHC bound peptides are drawn as a stick model (light yellow, carbon; dark yellow, sulfur; blue, nitrogen; red, oxygen). Hydrogen bonds are shown as dotted red lines and their distance is given in Å. Water molecule is shown as a red sphere.

Figure 9. 50 ns molecular dynamics simulation of the DQ2.5–CLIP1 complex. (left) Distance trajectories of several atom pairs in the $\alpha 22$ - $\alpha 24$ - $\alpha 31$ - $\beta 86$ - $\beta 90$ - $\alpha 9$ hydrogen bond network are shown; $O^{\epsilon 2}$ of $\beta 86E$ and $O^{\gamma 1}$ of $\beta 90T$ (green), $O^{\epsilon 1}$ of $\beta 86E$ and $O^{\epsilon 1}$ of $\alpha 31Q$ (cyan), $O^{\epsilon 1}$ of $\beta 86E$ and O^{η} of $\alpha 9Y$ (blue), $O^{\epsilon 1}$ of $\alpha 31Q$ and water (red), $N^{\delta 1}$ of $\alpha 24H$ and water (violet), and $N^{\epsilon 2}$ of $\alpha 24H$ and O^{η} of $\alpha 22Y$ (yellow). The black horizontal line at 3.5 Å demarcates the hydrogen bond threshold distance. (right) The hydrogen bonds are color coded and their distances measured from the crystal structure are indicated in Å.

Figure 10. Occupancy of the P1 pocket by $\alpha 51F$ in (a) DQ2.5–CLIP1–DM molecular dynamics simulation model, (b) mutant DQ2.5(E $\beta 86G$, Q $\alpha 31I$, H $\alpha 24F$)–CLIP1–DM molecular dynamics simulation model, and (c) DR1–HA–DM crystal structure (PDB ID: 4FQX).

Figure 11. Trajectory of the separation distance between $\alpha 51F$ (phenyl group centroid) and $\beta 82N$ (C^{α}) in the simulated wild-type and mutant DQ2.5–CLIP1–DM complexes.

Table 1. Data collection and refinement statistics

	DQ2.5-CLIP 1	DQ2.5-CLIP 2
Data collection		
Space group	C121	I23
Cell dimension		
a, b, c (Å)	128.86, 69.21, 146.69	137.01, 137.01, 137.01
α , β , γ (°)	90, 110.3, 90	90, 90, 90
Resolution (Å)	2.73	2.20
R_{merge}	10.0	12.9
$I/\sigma I$	11.7	12.7
Completeness %	93.7	99.65
Redundancy	3.5	6.5
Refinement		
Resolution (Å)	39.26 to 2.73 (2.80-2.73)	36.62-2.20 (2.30-2.20)
Number of reflections	29676	21938
$R_{\text{work}} / R_{\text{free}}$	0.187/0.247 (0.29-0.37)	0.171/0.208 (0.231-0.296)
Number of atoms	6144	3176
Protein	6027	3003
Water	117	173
B-factors	45.0	28.1
Protein	36.6	28.1
Water	28.1	29.3
r.m.s deviations		
Bond length (Å)	0.01	0.01
Bond angle (°)	1.24	1.12
Ramachandran	96.3	98.1

Values in parentheses are for highest resolution shell.

Figure 1.

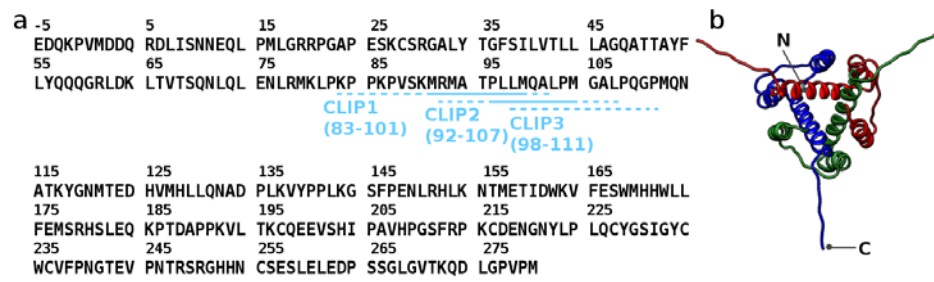


Figure 2.

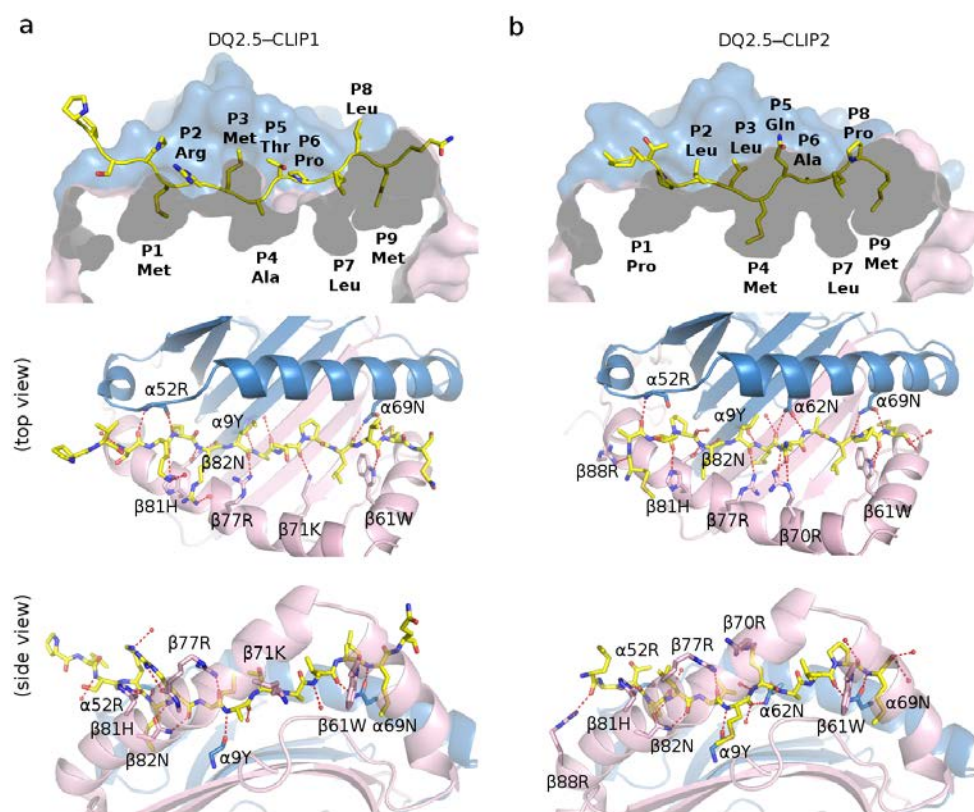


Figure 3.

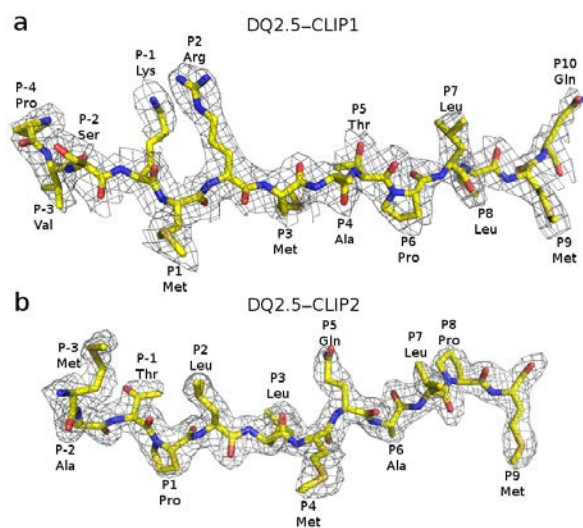


Figure 4.

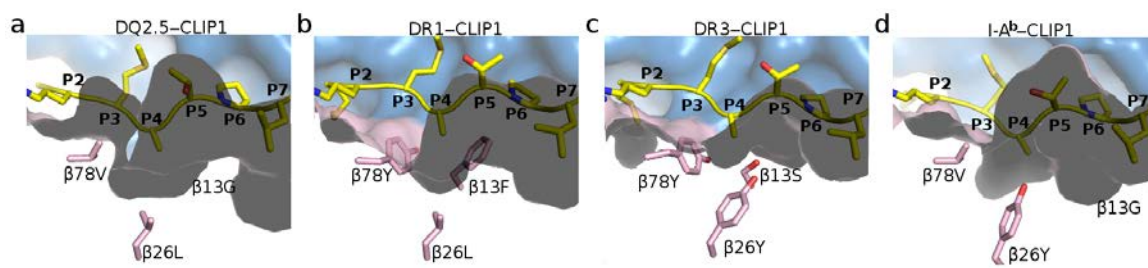


Figure 5.

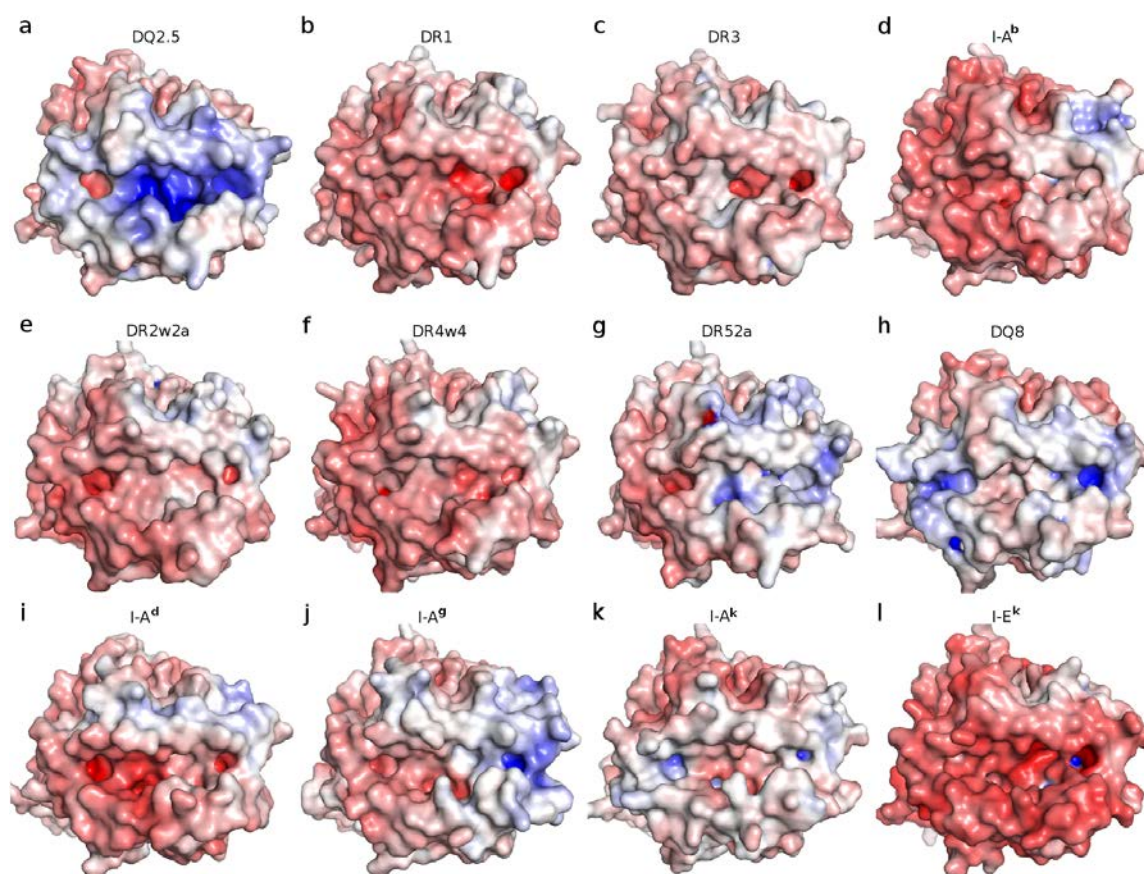


Figure 6.

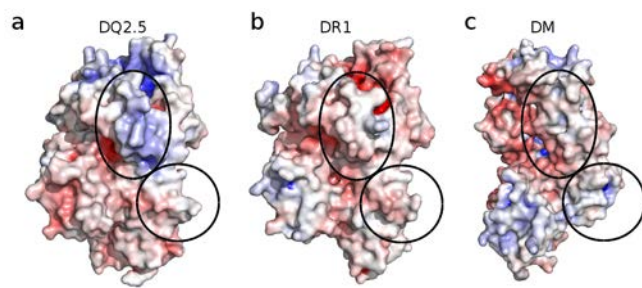


Figure 7.

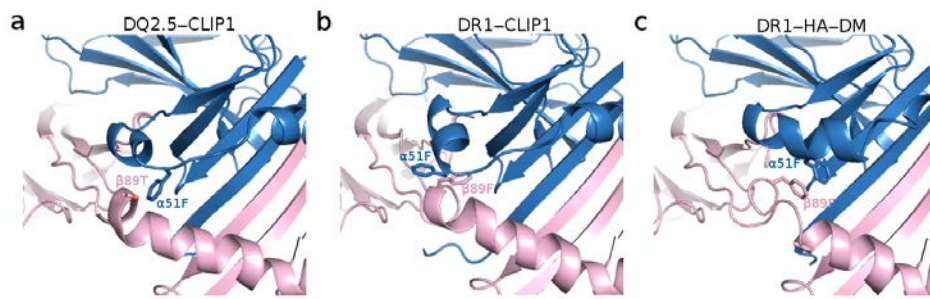


Figure 8.

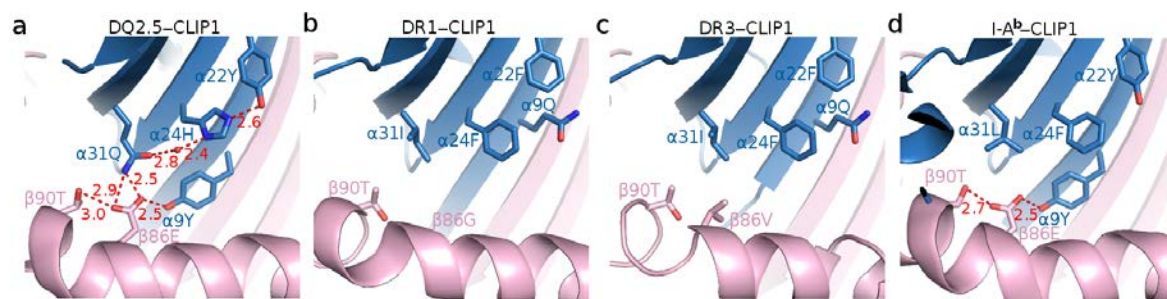


Figure 9.

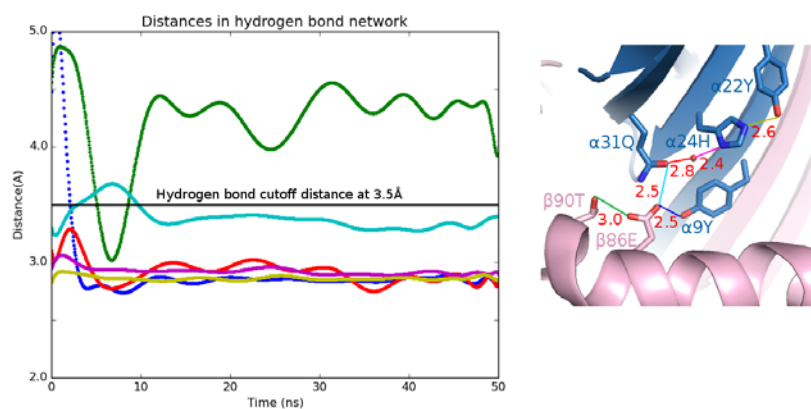


Figure 10.

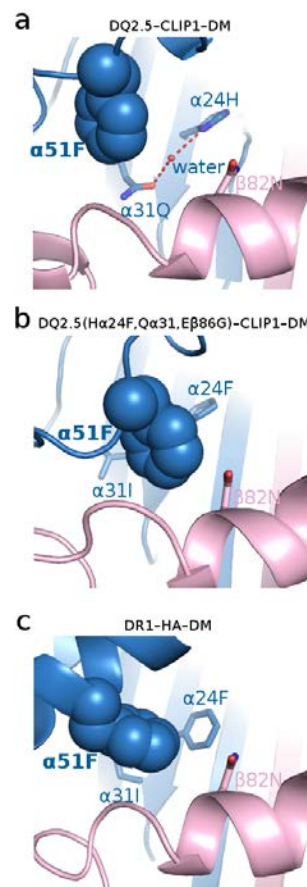
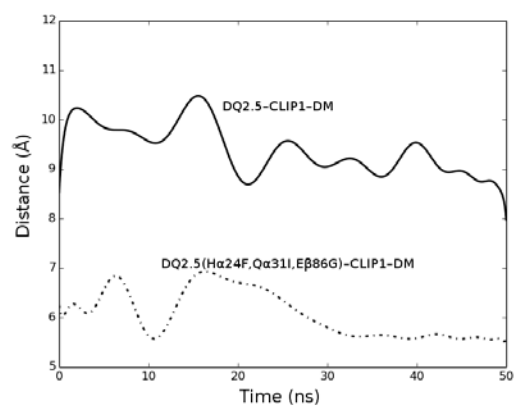


Figure 11.



Unraveling the structural basis for the unusually rich association of human leukocyte antigen DQ2.5 with class-II-associated invariant chain peptides
Thanh-Binh Nguyen, Priya Jayaraman, Elin Bergseng, Mallur S. Madhusudhan, Chu-Young Kim and Ludvig M Sollid

J. Biol. Chem. published online March 31, 2017

Access the most updated version of this article at doi: [10.1074/jbc.M117.785139](https://doi.org/10.1074/jbc.M117.785139)

Alerts:

- [When this article is cited](#)
- [When a correction for this article is posted](#)

[Click here](#) to choose from all of JBC's e-mail alerts

This article cites 0 references, 0 of which can be accessed free at
<http://www.jbc.org/content/early/2017/03/31/jbc.M117.785139.full.html#ref-list-1>